

# Synthesis, Characterization and Application of a Novel Zirconium Phosphonate Ion-Exchanger for Removal of Ni<sup>2+</sup>, Cu<sup>2+</sup> and Zn<sup>2+</sup> from Aqueous Solutions

*Faghihian, Hossein\*<sup>+</sup>*

*Department of Chemistry, Islamic Azad University, Shahreza Branch, Shahreza, I.R. IRAN*

*Yaghobb Nejadasl, Hooman*

*DDepartment of Chemistry, University of Isfahan, Isfahan, I.R. IRAN*

**ABSTRACT:** A new category of hybrid organic-inorganic zirconium phosphonate,  $Zr[(O_3PCH_2)_2NC_6H_4CO_2H].2H_2O$  was synthesized and the applicability of the prepared sorbent as an ion-exchanger for removal of Ni<sup>2+</sup>, Cu<sup>2+</sup> and Zn<sup>2+</sup> from aqueous solutions was evaluated. The characterization of the synthesis product was done using TG-DTG, SEM, XRD, FT-IR techniques. Study of the sorption isotherms and its kinetic parameters was performed by atomic absorption spectroscopy and potentiometric techniques respectively. The adsorbent showed very high sorption rate and good adsorption capacity. Based on the high sorption rates, a typical ion exchange chromatography separation was performed using a column packed with the synthesized ion-exchanger and the results are discussed.

**KEY WORDS:** Zirconium phosphonate, Sorption isotherm, Ion exchange, Chromatography separation.

## INTRODUCTION

Zirconium phosphonates belongs to the class of hybrid organic inorganic materials and are organic derivatives of zirconium phosphates. The general formula describing zirconium phosphonates is  $Zr(O_3PR)_2.nH_2O$ , in which R is an organic radical. The nature and diversity of the organic group that could be inserted in interlayer space made zirconium phosphonates as highly potential materials for different applications. An accurate control of the dimensions and reactivity of the interlayer space is possible by selecting

the appropriate organic group R [1]. The different applications that emerge from such modifications include: intercalation of guest molecules [2], ion selective materials, ion-gates [3], photophysical reactions inside zirconium phosphonates structures [4], fabricating of sensors and bio-sensors [5,6], designing protonic conductors for fuel cell membranes [7], selective catalysis [8] and bio-consistent beds for studying photo-biological reactions [9].

---

\* To whom correspondence should be addressed.

+E-mail: h.faghihi@sci.ui.ac.ir

1021-9986/11/2/23

9/\$/2.90

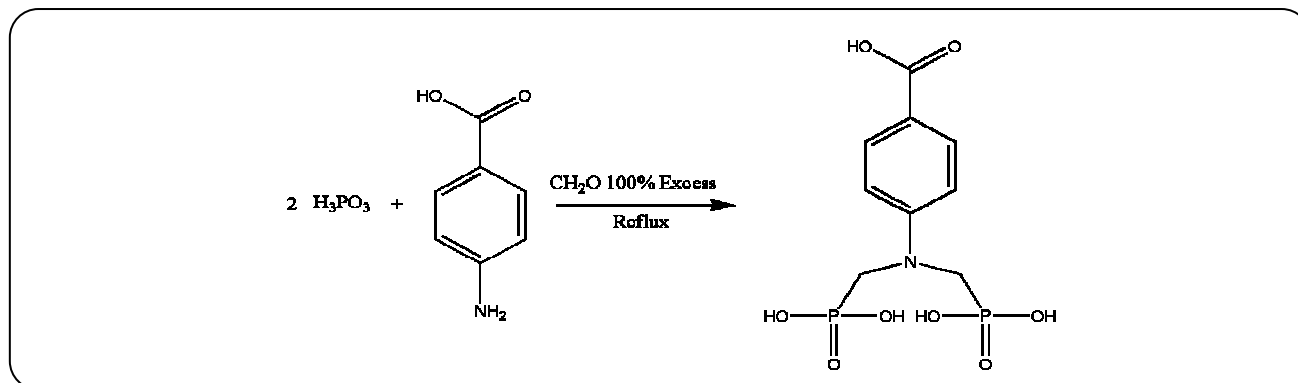


Fig. 1: Synthesis of 4-carboxyphenylamino-bis-phosphonic acid.

By a survey of the literature it is evident that little research works have been done in the field of zirconium phosphonate as ion exchangers. Indeed most of the workers have used zirconium phosphonates with strong acid behavior for this aim and the lack of data on the function and application of other types of zirconium phosphonate is sensible. The present study attempts to explore the possibility of synthesis and application of a zirconium phosphonate with weak Lewis acid exchanger groups for the separation of  $\text{Ni}^{2+}$ ,  $\text{Cu}^{2+}$  and  $\text{Zn}^{2+}$  cations. The aim of this work was to utilize structural capabilities of a given zirconium diphosphonate in conjunction with its ion-exchange behavior in order to reach to a compromise between thermodynamic and kinetic parameters for ion exchange separation of the cations. Finally, a demonstrative chromatographic separation will be presented by using the synthesized material and its possible uses in the field of ion exchange chromatography will be evaluated.

## EXPERIMENTAL SECTION

### Reagents

All of the chemicals used were the product of Merck/Germany and of synthesis grade.

### Synthesis procedures

#### Preparation of diphosphonic acid

The 4-carboxyphenylamino-bis-methylphosphonic acid,  $(\text{H}_2\text{O}_3\text{PCH}_2)_2\text{NC}_6\text{H}_4\text{CO}_2\text{H}$  was synthesized according to the method explained by Moedritzer-Irani [10].

31.5 mL  $\text{H}_3\text{PO}_3$  30% (0.1 mol) and 27.4 g (0.2 mol) 4-amino benzoic acid were mixed in 50 mL of hydrochloric acid solution with  $[\text{H}^+]/[\text{amine}]=2\sim 3$ . The mixture was allowed to be refluxed for 3h while 60 mL of methanal

37% solution (0.4mol; 100% excess) was added drop wise to the reaction mixture.

The post synthesis product was a very viscose liquid mixture that resist against crystallization and hence the purification of the synthesized diphosphonic acids was somehow difficult and inefficient. This mixture contains the diphosphonic acids as well as starting materials. Since no interference would be expected from the starting materials on the final zirconium phosphate function, the obtained diphosphonic acid was used in the preparation of zirconium phosphonate without any further purification.

#### Preparation of Zirconium 4-carboxyphenylamino-bis-methylphosphonate.dihydrate

##### $\text{Zr}[(\text{O}_3\text{PCH}_2)_2\text{NC}_6\text{H}_4\text{CO}_2\text{H}].2\text{H}_2\text{O}$

The synthesized diphosphonic acid was dissolved in 50 mL of hydrochloric acid (pH=1) and added to the  $\text{Zr}^{4+}$  solution prepared by solving 23.3 g (0.1 mol) of  $\text{ZrCl}_4$  in water. The mixture was stirred for 3~4 h at 60~70 °C. The reaction scheme is shown in Fig.2.

The solid product was then separated by centrifugation at 3400 rpm for 10 min and washed with water to pH=5 and then dried in oven for 24 h at 105 °C, followed by grinding to the desired particle size. For recording XRD pattern of the synthesized sorbent, the crystalline structure of the product must be enhanced. For this reason 0.5 g of the product was placed in contact with 7 mL HF 38% solution (F/Zr=15) in a Teflon lined stainless steel autoclave and placed in an oven for two weeks at 170 °C and then filtered, washed with water and dried at 105 °C for 24 h.

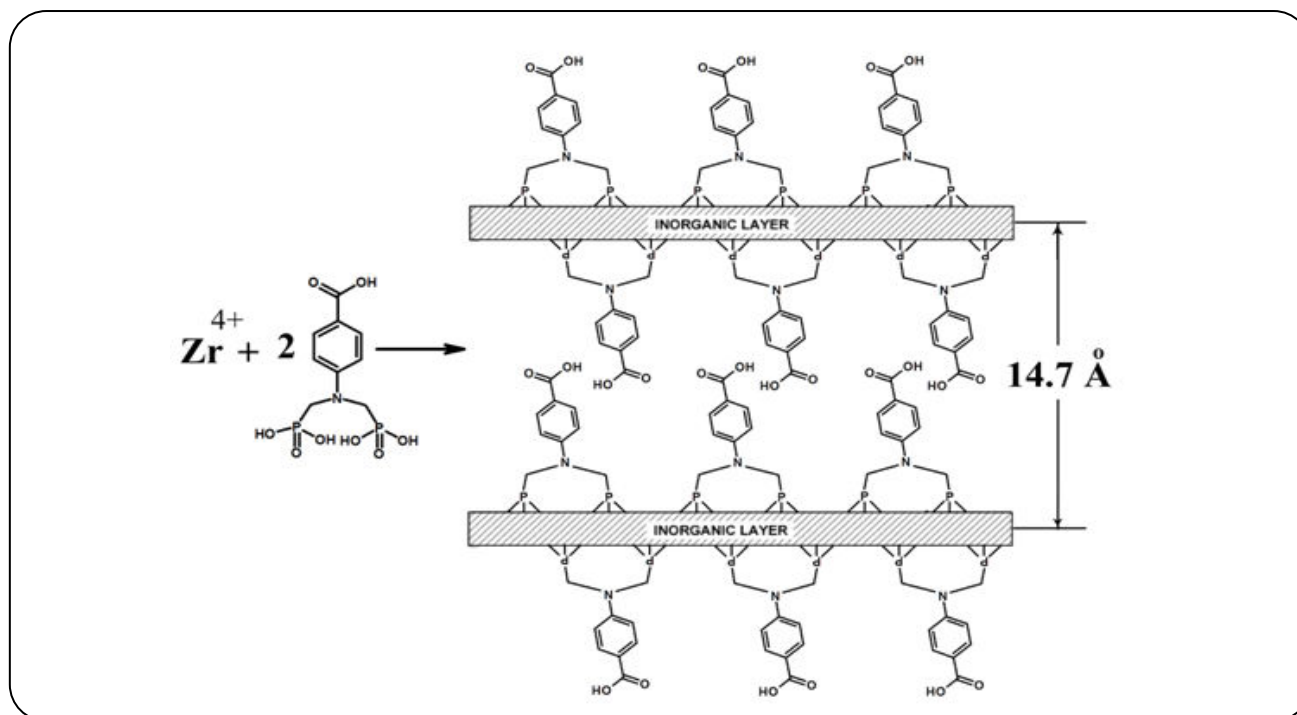


Fig. 2: Synthesis scheme of zirconium bis-phosphonate.

#### Instrumental procedures

DTG analysis was performed with a TA4000 Mettler System with initial temperature of 25 °C, end temperature 800 °C and heating rate of 5 °C min<sup>-1</sup> upon atmospheric conditions. The infrared spectrum of the sample recorded using an Impact 400D Nicolet FT-IR spectrometer. powder X-Ray Diffraction (XRD) pattern was obtained using a D8ADVANCE Bruker diffractometer, at Cu K $\alpha$  ( $\lambda=1.5405$  Å). SEM micrographs for morphological characterizations were obtained using XL30Philips SEM instrument. The concentration of Ni<sup>2+</sup>, Cu<sup>2+</sup> and Zn<sup>2+</sup> prior and after adsorption was determined by atomic absorption spectroscopy using an atomic absorption AA670 Shimadzu spectrometer. For kinetic evaluation of sorption process and recording chromatographic elution curves of metal ions a pH Lab 827 Metrohm potentiometer was used in which potential was monitored over time which uses a S.C.E reference electrode and a first kind indicator electrode made of the metal wire of the ion under consideration.

#### Adsorption isotherms

Determination of the adsorption isotherms was performed by batch method. Typically, 20 mL cation

solution (50 to 1500 ppm) was put in contact with 0.2 g of the sorbent in polyethylene bottles and then placed in a shaker bath at desired temperatures for a day.

#### Kinetics of the sorption

For determination of mechanism of sorption 40 mL of the cation solution was placed in contact with the first type potentiometric electrodes while stirring. The stirring rate was the same in all cases. After fixation of the potential 0.4 g of the sorbent was added to the metal ion solution and then the potential as a measure of the concentration of the cation was recorded over time. All of the measurements were done in a bath with constant temperature of 303 K.

#### Chromatography separations

For chromatographic separation of the mentioned metal ions a packed column using the synthesized sorbent with particle diameter of 50  $\mu\text{m}$  was prepared. The dimensions of the column include:  $h=8.5$  cm,  $i.d=1.3$  cm. Elution was performed in isocratic mode using HNO<sub>3</sub> solution of pH 2.5. Injection of the sample was performed using an Eppendorf 2.5 mL fixed-volume pipette. The injected sample contained 200 ppm Ni<sup>2+</sup>, 200 ppm Cu<sup>2+</sup> and 150 ppm Zn<sup>2+</sup>. The flow rate of the mobile phase

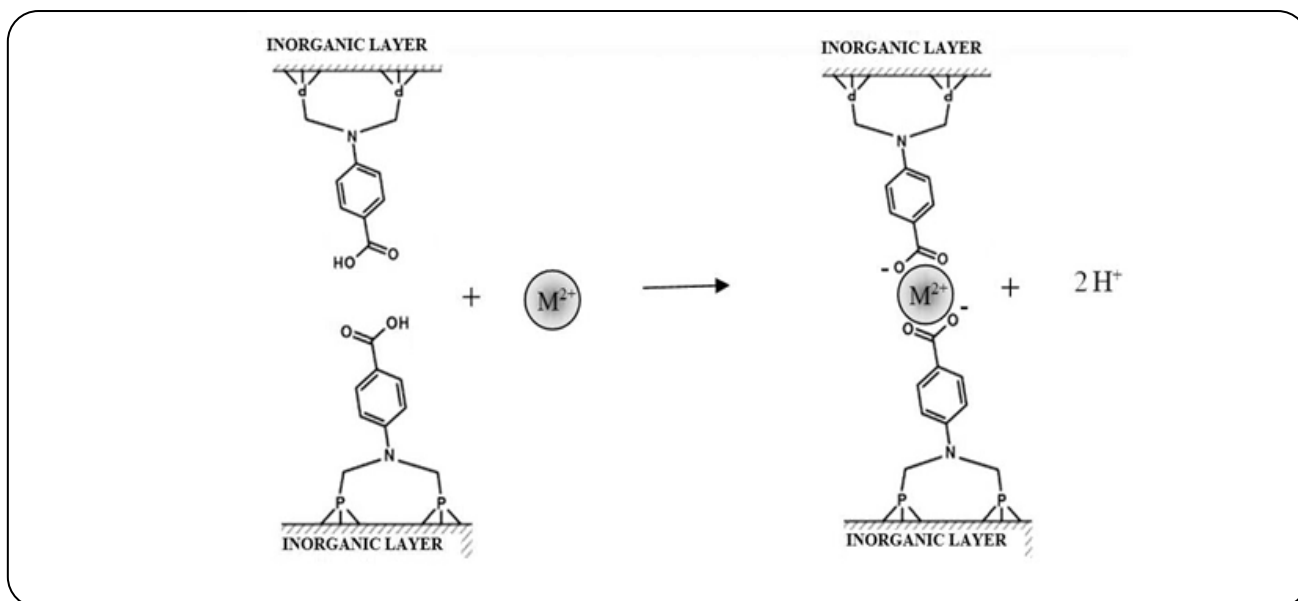


Fig. 3: Depiction of the ion-exchange process in the interlayer space of the zirconium 4-carboxyphenylamino-bis-methylphosphonate.

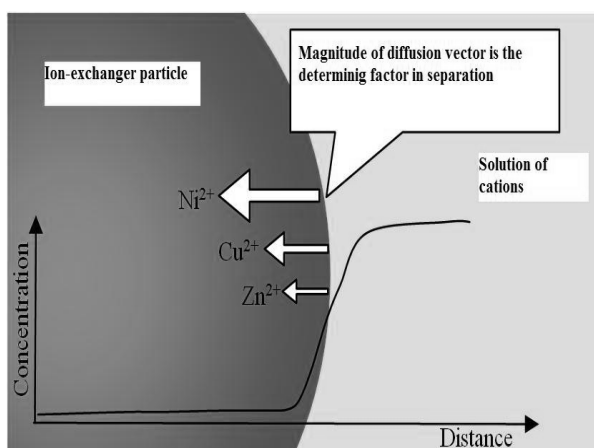


Fig. 4: Schematics of Drag-force of the synthesized material toward diffusion of the three ions under study.

and the temperature of the columns were  $0.023 \text{ mL}\cdot\text{sec}^{-1}$ , and  $303 \text{ K}$  respectively. Detection was done using the potentiometric system at the end of the column with metallic wire of each metal ion and a S.C.E reference electrode.

## RESULTS AND DISCUSSION

### Zirconium 4-carboxyphenylamino-bis-methylphosphonate

Zirconium phosphonate with weak acid exchange sites has been less applied for ion-exchange separations. This is mainly due to the loss of the exchange capacity. However, it should be noted that a loss in exchange

capacity is a problem if the whole process is going to be performed via pure thermodynamic ion-exchange; in other words, if the mechanism of the separation process is based on a kinetically controlled diffusion of ions inside the ion-exchanger materials, the loss of ion-exchange capacity will not interfere too a great extend.

Here, the strategy was to design a zirconium phosphonate ion-exchanger which allows high sorption rates, so that the differences in sorption rates are the major factor that causes separation of different cations from each other. Obviously, the ion-exchange sites inside the zirconium phosphonate particles exchange the incoming ions of the solution with the  $\text{H}^+$  ions of the weak exchange sites (Fig. 3). This sorption creates a concentration gradient inside the zirconium phosphonate phase, which is the force required for the ions to diffuse further into the sorbent particle. The resistance of the zirconium phosphonate structure toward diffusion of different cations causes each ion has a diffusion coefficient different from other ions (Fig. 4). This difference in diffusion rates is the basis of separation in Zirconium 4-carboxyphenylamino-bis-methylphosphonate (c.f. chromatography separation section).

Three factors affect the sorption rates in the case of lamellar structures: the interlayer distance [12], the steric hindrance within the layer [11], and the grain size of the particles. The first and second factors were provisioned in the design and synthesis of the biphosphonic acid.

This includes the involvement of an aromatic ring in the body of the biphosphonic acid. Since aromatic rings are rigid, they will push the layers apart and provide more space for diffusing cations in the interlayer space. Also by using a biphosphonic acid, only one exchange site is associated to the two phosphonate terminals and this result in decrease of the steric hindrance within the layer to 50% (Figs. 1 and 2).

#### Thermogravimetric Analysis

TG and DTG patterns of the prepared zirconium phosphonate sample are shown in Fig. 5. Two weight loss steps are observed, one starting at about 50 °C and peak centered at about 100 °C ascribed to loss of adhered and intercalated water and the other peak starts at about 300 °C and peak centered at 450 °C is due to destruction of the organic functional moiety. From the thermal curves it could be concluded that it synthesized product could be used safely below 300 °C.

#### XRD results

The XRD patterns were typical of layered compounds being characterized by a strong peak at low  $2\theta$  values (which can be associated with the scattering of dense layer planes) and other much less intense peaks at higher  $2\theta$  values. Accordingly, the  $d$  values of the first intense diffraction peak represent the interlayer distances of the compounds and hence the  $d$  values can be used for verification of placement of functional groups between zirconium layers. As can be seen from the XRD patterns (Fig. 6), the interlayer distances has increased from 7.6 Å in original zirconium phosphate to about 14.7 Å in the modified zirconium phosphonate structure.

#### FT-IR spectra

The FT-IR spectrum of zirconium 4-carboxyphenylamino-bis-methylphosphonate is shown in Fig. 7.

The peak at  $567\text{ cm}^{-1}$  is due to Zr-O stretching, strong absorption between  $900\sim 1100\text{ cm}^{-1}$  is assigned to the stretching modes of  $\text{O}_3\text{P}$ , the absorption bands at  $3430$  and  $1640\text{ cm}^{-1}$  arise from stretching and bending vibrations of intercalated water respectively. The strong peak at  $1382\text{ cm}^{-1}$  is ascribed to the P-CH<sub>2</sub> bending that could be taken advantage for confirming the formation of a bond between phosphorus acid and methanal. The peaks at  $1510$  and  $1604\text{ cm}^{-1}$  are vibrations of aromatic ring and one at  $1707\text{ cm}^{-1}$  is due to the stretching vibration of

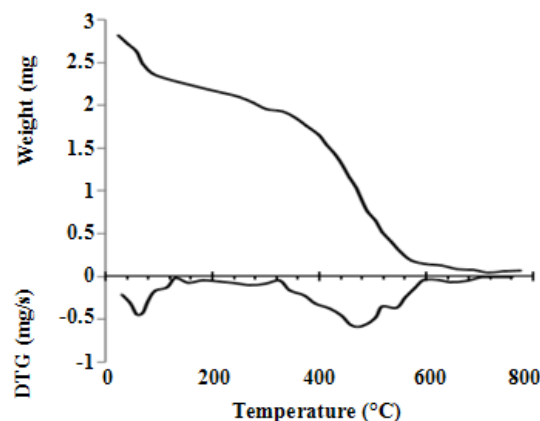


Fig. 5: TG and DTG curves of zirconium 4-carboxyphenylamino-bis-methylphosphonate.

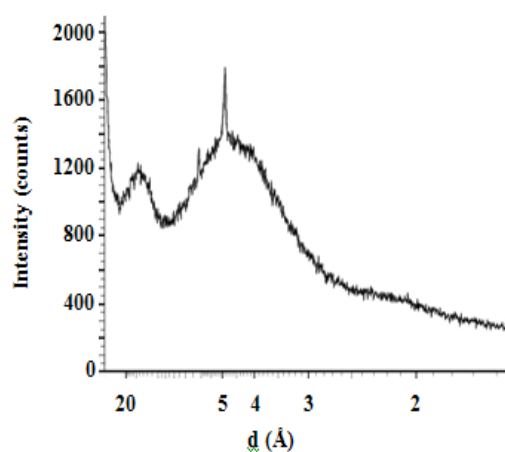


Fig. 6: XRD pattern of zirconium 4-carboxyphenylamino-bis-methylphosphonate.

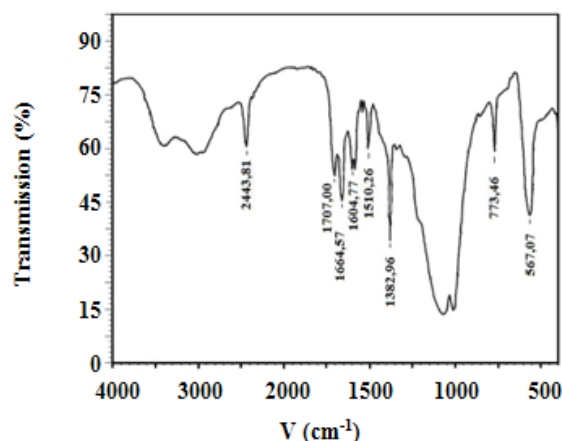


Fig. 7: FT-IR spectrum of zirconium 4-carboxyphenylamino-bis-methylphosphonate.

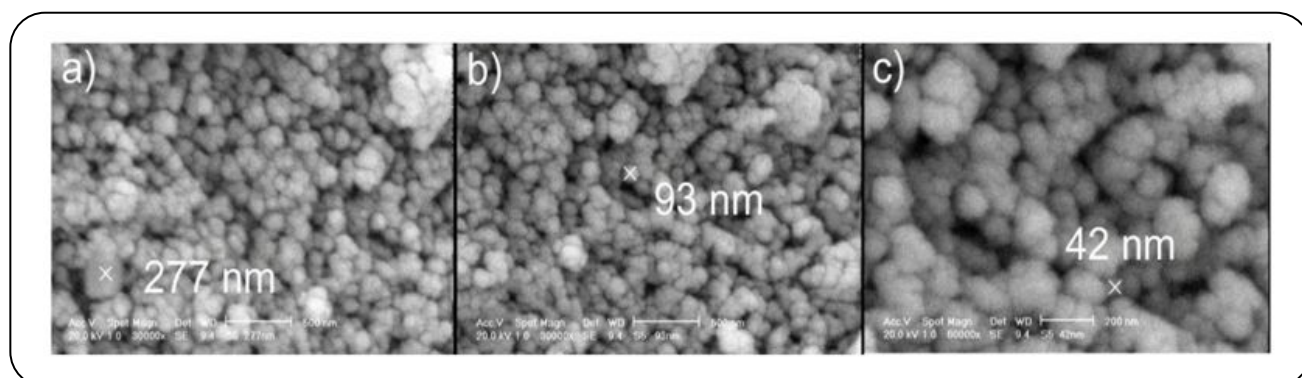


Fig. 8: SEM micrographs of synthesized zirconium biphosphonate sample; a) and b), 30000x; c) 60000x.

carbonyl of carboxylic acid. The broad absorption band from 2400~3400  $\text{cm}^{-1}$  arise from stretching of acidic -OH of carboxylic acid group.

#### Morphological Characterization of Zirconium Phosphonate

The SEM micrographs of zirconium 4-carboxyphenylamino-bis-methylphosphonate are shown in Fig. 8. It was found that the sorbent comprises particles with diameters in the 42~277 nm range. The amorphous and microporous structure greatly increased the surface area and the accessibility for substrates to the acid sites. Also, the nanometric particles greatly enhance the sorption rate.

#### Sorption Isotherms

In order to evaluate a mathematical relationship to describe the sorption of cations by zirconium phosphonate, the experimental data was fitted with a sorption isotherm equation. In this case Freundlich sorption isotherm was the one that best fitted with the experimental data. The Freundlich isotherm (1906) is expressed by the following linearized equation [13]:

$$\text{Log } Q_e = \text{Log } K_F + (n) \text{Log } C_e \quad (1)$$

Where  $Q_e$  and  $C_e$  are equilibrium equivalent sorbed and equilibrium sorption concentration of adsorbate respectively and  $K_F$  and  $n$  are empirical constants associated with strength of interaction between adsorbent and adsorbates.

Accordingly, the plot of  $\text{Log } Q_e$  versus  $C_e$  at each temperature should give a straight line. The values of  $R^2$  give a measure of the applicability of the model postulated for the sorption process under study.

The  $Q_e$  versus  $C_e$  curves for  $\text{Ni}^{2+}$ ,  $\text{Cu}^{2+}$  and  $\text{Zn}^{2+}$  have been shown in Fig. 9 to Fig. 11 respectively.

The correspondence of the sorption isotherm curves with Freundlich sorption model is shown in Table 1.

The high sorption capacity of the prepared sorbent represented in the curves toward the studied cations is interesting.

From the high capacity of the sorbent for sorption of  $\text{Zn}^{2+}$  ions ( $\text{Zn}^{2+}$  loading values in Fig. 11), the selectivity of the synthesized structure toward these cations is obvious. The three transition metal ions were selected so that the effect of physical parameters on the sorption process was minimized. This includes the size of hydrated ion and electrostatic charge located on each. Thus the higher sorption capacity in the case of zinc ions could be a consequence of electronic interactions and complex formation inside the zirconium phosphonate phase.

#### Kinetic behavior

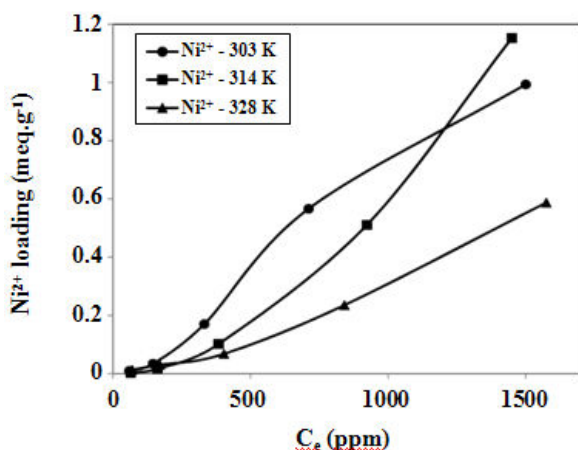
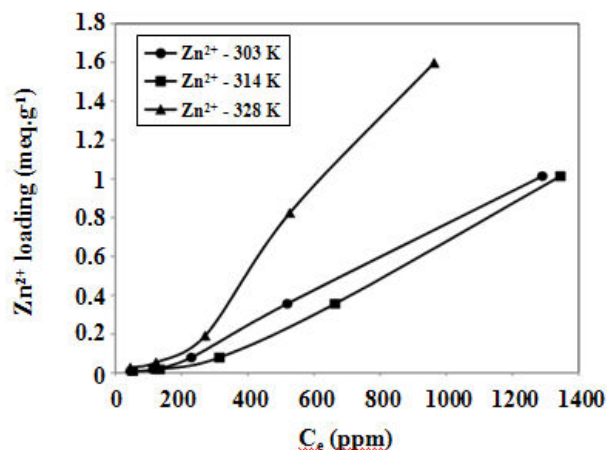
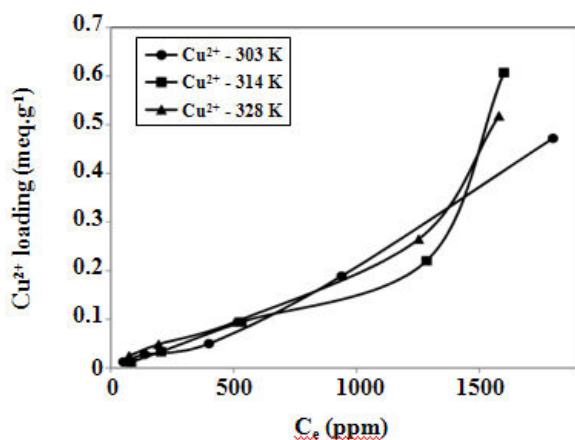
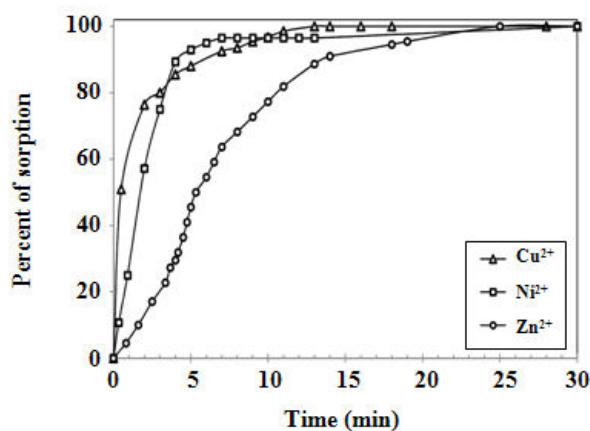
The kinetic curves displaying the sorption rate for each ion is depicted in Fig. 12.

The result of kinetic experiments showed relative high sorption rates that were not observed previously in the case of zirconium phosphate and its derivatives. The rate of sorption has been increased markedly for all of the metal ions under study relative to sorption of transition metals onto amorphous zirconium phosphate [14,15].

Comparison of the rate of sorption with ionic radii of these transition metal ions reveals that the ionic species diffuse inside the zirconium phosphonate phase while completely or partly lost their hydration sphere ( $\text{Ni}^{2+}=70$ ,  $\text{Cu}^{2+}=73$ ,  $\text{Zn}^{2+}=75$  pm). Thus it is concluded that sorption rate has a size dependent mechanism.

Table 1: Freundlich sorption isotherm parameters for  $\text{Ni}^{2+}$ ,  $\text{Cu}^{2+}$  and  $\text{Zn}^{2+}$ .

Temperature (K)	Cation								
	$\text{Ni}^{2+}$			$\text{Cu}^{2+}$			$\text{Zn}^{2+}$		
	$K_F$	$n$	$R^2$	$K_F$	$n$	$R^2$	$K_F$	$n$	$R^2$
303	$6.99 \times 10^{-4}$	1.5	0.984	$6.28 \times 10^{-3}$	1.0	0.962	$6.56 \times 10^{-4}$	1.5	0.980
314	$3.58 \times 10^{-5}$	1.9	0.999	$1.75 \times 10^{-3}$	1.2	0.967	$1.29 \times 10^{-3}$	1.4	0.972
328	$1.89 \times 10^{-3}$	1.2	0.980	$1.16 \times 10^{-2}$	0.9	0.959	$2.66 \times 10^{-3}$	1.4	0.967

Fig. 9: Sorption isotherms of  $\text{Ni}^{2+}$ .Fig. 11: Sorption isotherms of  $\text{Zn}^{2+}$ .Fig. 10: Sorption isotherms of  $\text{Cu}^{2+}$ .Fig. 12: Sorption rates of  $\text{Ni}^{2+}$ ,  $\text{Cu}^{2+}$  and  $\text{Zn}^{2+}$  on zirconium 4-carboxyphenylamino-bis-methylphosphonate.

As the sorption process has activation energy dependent on the interlayer space, it is evident that increasing the interlayer distance would end up in higher rates of sorption process.

### Chromatography Separation

Based on the data obtained in thermodynamic and kinetic study of Zirconium 4-carboxyphenylamino-bis-

methylphosphonate an ion exchange column chromatographic separation was designed to evaluate the overall separation capability of the synthesized zirconium phosphonate material from both ion-exchange and diffusion aspects. The elution curves of  $\text{Ni}^{2+}$ ,  $\text{Cu}^{2+}$  and  $\text{Zn}^{2+}$  are shown in Fig. 13.

As could be seen from the chromatogram, in this case the kinetic factors are dominant in chromatographic separation; say, the order of elution of each metal ion

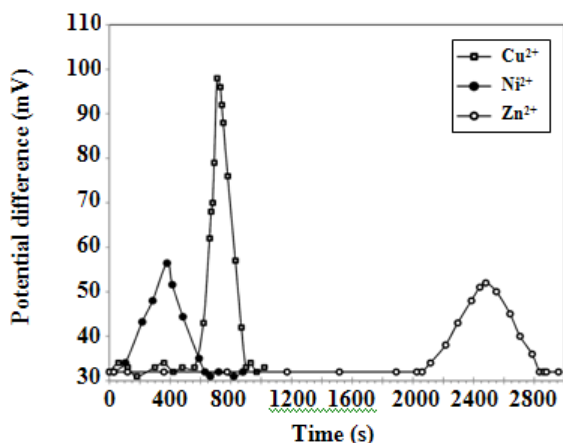


Fig. 13: Chromatographic separation of  $Ni^{2+}$ ,  $Cu^{2+}$  and  $Zn^{2+}$  at  $T=303\text{ K}$ .

component is the reverse of the order of kinetic sorption rate. Therefore it could be concluded that the ion with the smallest ionic radii would have the fastest diffusion rate inside the sorbent phase and will be eluted latest. Although this is the kinetic parameters that determine general aspects of separation, thermodynamic parameters could affect the shape of the peaks. The peak broadening that is observed in the case of  $Zn^{2+}$  ions is a result of the relative high tendency of the zirconium phosphonate to these ions. However since zinc ions have to be exchanged with hydrogen ions, this is possible to control the amount of peak broadening by adjusting the pH of the mobile phase.

The most notable characteristics of the weak Louis acid groups that were used for modification of zirconium phosphonate is that since all of the weak acid groups has a intrinsic tendency toward sorption of  $H^+$  ions, no other cation could be sorbed most favorable than  $H^+$  ions under normal conditions. Unlike zirconium phosphates modified by strong Louis acid groups, this will leads to more moderate behavior of the sorbent toward adsorbates. As shown in the case of  $Zn^{2+}$  ions, when a relative strong tendency exists for sorption of a component, the chromatograph shows some kinds of peak broadenings.

## CONCLUSIONS

The preparation scheme, characterization and sorption process of nanoparticles of a hybrid organic inorganic zirconium phosphonate with weak ion-exchange properties toward  $Ni^{2+}$ ,  $Cu^{2+}$  and  $Zn^{2+}$  ions have been considered for the first time in which diphosphonic acids was used as building blocks. The aim was to examine the effect

of diphosphonic acids that act as multifunctional groups: spacer, ion-exchanger and supplier of more space for diffusing adsorbates through sorbent by reducing hindrance. From the results it was evident that the turnover of the prepared hybrid material was superb in both thermodynamic and kinetic aspects of views. The results have shown that the separation was done almost on kinetic basis, while thermodynamic characteristics affect peak shapes in chromatographs.

Therefore it could be concluded that zirconium phosphonate with weak acid properties are good for packed column chromatography separations, since they provide for a reasonable combination of retention factor and resolution; however in the case of batch operations, zirconium phosphonate with strong acid groups seems to be more useable due to their higher capacity of sorption.

The effect of other phosphonic acids with different geometrical-chemical properties in this field seems interesting.

Received : Jan. 27, 2009 ; Accepted : Sep. 5, 2010

## REFERENCES

- [1] Alberti G., Costantino U., Vivani R., Zappelli P., Zirconium Phosphite (3,3',5,5'-Tetramethylbiphenyl)diphosphonate, a Microporous, Layered, Inorganic–Organic Polymer, *Angew. Chem., Int. Ed. Engl.*, **32**, p. 1357 (1993).
- [2] Clearfield A., Poojary D.M., Zhang B., Zhao B., Derecskei-Kovacs A., Azacrown Ether Pillared Layered Zirconium Phosphonates and the Crystal Structure of *N,N'*-Bis(phosphonomethyl)-1,10-diaza-18-crown-6, *Chem. Mater.*, **12**, p. 2745 (2000).
- [3] Zhang B., Clearfield A., Crown Ether Pillared and Functionalized Layered Zirconium Phosphonates: A New Strategy to Synthesize Novel Ion Selective Materials, *J. Am. Chem. Soc.*, **119**, p. 2751 (1997).
- [4] Vermeulen L.A., Thompson M.E., Synthesis and Photochemical Properties of Porous Zirconium Viologen Phosphonate Compounds, *Chem. Mater.*, **6**, p. 77 (1994).
- [5] Alberti G., Casciola M., Palombari R., Inorgano-Organic Proton Conducting Membranes for Fuel Cells and Sensors at Medium Temperatures, *J. Membr. Sci.*, **172**, p. 233 (2000).

- [6] Monot J., Petit M., Lane S.M., Guisle I., Léger J., Tellier Ch., Talham D.R., Bujoli B., Towards Zirconium Phosphonate-Based Microarrays for Probing DNA-Protein Interactions: Critical Influence of the Location of the Probe Anchoring Groups, *J. Am. Chem. Soc.*, **130**, p. 6243 (2008).
- [7] Dagani R., Putting the 'NANO' into Composites, *Chem. Eng. News.*, **77**, p. 25 (1999).
- [8] Doughty, S.K., Simpson, G.J., Rowlen, K.L., Evolution of Orientation in the Growth of Azo Dye Zirconium Phosphate-Phosphonate Multilayers, *J. Am. Chem. Soc.*, **120**, p. 7997 (1998).
- [9] Martí A.A., Paralitici G., Maldonado L., Colón J.L., Photophysical Characterization of Methyl Viologen Ion-Exchanged Within a Zirconium Phosphate Framework, *Inorg. Chim. Acta*, **360**, p. 1535 (2007).
- [10] Moedritzer K., Irani, A., The Direct Synthesis of  $\alpha$ -Aminomethylphosphonic Acids. Mannich-Type Reactions with Orthophosphorous Acid, *J. Org. Chem.*, **31**, p. 1603 (1966).
- [11] Loukah M., Condurier G., Vedrine J.C., Ziyad M., Oxidative Dehydrogenation of Ethane on V- and Cr-Based Phosphate Catalysts, *Microporous Materials*, **4**, p. 345 (1995).
- [12] Vivani R., Alberti G, Costantino F, Nocchetti M., New Advances in Zirconium Phosphate and Phosphonate Chemistry: Structural Archetypes, *Microporous Mesoporous Mater.*, **107**, p. 58 (2008).
- [13] Perry R.H., Green D., "Perry's Chemical Engineer's Handbook", 7th Edition, McGraw-Hill, (1999).
- [14] Zhang Q.R.; Du W., Pan B.C., Pan B.J., Zhang, W.M., Zhang Q.J., Xu Z.W., Zhang Q.X., A Comparative Study on  $Pb^{2+}$ ,  $Zn^{2+}$  and  $Cd^{2+}$  Sorption onto Zirconium Phosphate Supported by a Cation Exchanger, *J. Hazard. Mater.*, **152**, p. 469 (2008).
- [15] Jiang P., Pan B.C., Pan B.J., Zhang W., Zhang, Q., A Comparative Study on Lead Sorption by Amorphous and Crystalline Zirconium Phosphates Colloids, *Surf., A*, **322**, p. 108 (2008).